MOLECULAR BIOLOGY

The adenine nucleotide translocase family underlies cardiac ischemia-reperfusion injury through the mitochondrial permeability pore independently of cyclophilin D

Pooja Patel[1]†, Arielys Mendoza[1]†, Daniel Ramirez[1], Dexter Robichaux[1], Jeffery D. Molkentin[2], Jason Karch[1,3]*

The mitochondrial permeability transition pore (mPTP) is implicated in cardiac ischemia-reperfusion (I/R) injury. During I/R, elevated mitochondrial Ca^{2+} triggers mPTP opening, leading to necrotic cell death. Although nonessential regulators of this pore are characterized, the molecular identity of the pore-forming component remains elusive. Two of these genetically verified regulators are cyclophilin D (CypD) and the adenine nucleotide translocase (ANT) family. We investigated the ANT/CypD relationship in mPTP dynamics and I/R injury. Despite lacking all ANT isoforms, Ca^{2+}-dependent mPTP opening persisted in cardiac mitochondria but was desensitized. This desensitization conferred resistance to I/R injury in ANT-deficient mice. CypD is hypothesized to trigger mPTP opening through isomerization of ANTs at proline-62. To test this, we generated mice that expressed a P62A mutated version of ANT1. These mice showed similar mPTP dynamics and I/R sensitivity as the wild type, indicating that P62 is dispensable for CypD regulation. Together, these data indicate that the ANT family contributes to mPTP opening independently of CypD.

INTRODUCTION

The opening of the mitochondrial permeability transition pore (mPTP) is a major contributing factor to cardiac ischemia-reperfusion (I/R) injury (*1*). The mPTP is an unidentified nonselective pore that resides within the inner mitochondrial membrane and is activated by increased matrix Ca^{2+} (*2*). Regulators of this pore include cyclophilin D (CypD), the Bcl-2 family, and the adenine nucleotide translocase (ANT) family (*3*–*5*). CypD is a *cis-trans* peptidyl-prolyl isomerase (PPIase) that resides in the mitochondrial matrix (*6*). Genetic deletion or pharmacological inhibition of CypD desensitizes the mPTP to Ca^{2+}-dependent opening and decreases the infarct size in animal models subjected to I/R injury (*7*, *8*). Deletion of proapoptotic Bcl-2 family members BAX and BAK1 inhibits Ca^{2+}-dependent mitochondrial swelling and leads to a reduction in infarct size in mice following I/R injury (*4*, *9*, *10*). The ANT family is responsible for transporting adenosine diphosphate (ADP) into the mitochondrial matrix and adenosine triphosphate (ATP) into the intermembrane space (*11*). Originally, the ANT family was thought to be the pore-forming component of the mPTP due to inhibitors and substrates of the family having severe effects on mPTP kinetics. In addition, because of its association with CypD, it has been speculated that CypD is able to trigger mPTP opening through the ANT family, specifically at the highly conserved proline-62 within the first matrix facing loop of the ANT (*12*). However, genetic deletion of the ANT family in the liver revealed that they are not essential for mPTP opening to occur (*13*, *14*). Recently, we showed that the loss of the ANT family coupled with the loss or inhibition of CypD completely blocks mPTP opening in liver mitochondria, suggesting the existence of two distinct mechanisms of permeability transition (*13*). This "two-pore" hypothesis was pursued and affirmed in skeletal muscle mitochondria in context to muscular dystrophy. Dystrophic mice lacking ANT1 have reduced cell death, and cell death is further reduced in dystrophic mice lacking both ANT1 and CypD (*15*).

Here, we genetically removed all isoforms in the ANT family in the heart and found that cardiac ANT-null (ANT-cTKO) mitochondria have a greater Ca^{2+} retention capacity (CRC) than controls and the CRC was further increased when treated with CypD inhibitor, cyclosporine A (CsA). In addition, ANT-cTKO mice have reduced infarct size compared to controls following I/R injury. Furthermore, wild-type (WT) and ANT2-only expressing mice treated with CsA were less resistant to I/R injury than cTKO mice treated with CsA. To determine whether CypD could regulate the mPTP through P62 within the ANT, we generated ANT1P62A expressing mice ($ANT1^{P62A/P62A}$). We found that proline-62 is dispensable for CypD-dependent mPTP activation. Mice and mitochondria only expressing this mutant version of ANT1 were still responsive to CypD inhibition through CsA measured by infarct size reduction and mPTP desensitization.

RESULTS

Inhibition of the mPTP through the ANT family and CypD regulators increases the CRC in cardiac mitochondria

Recently, we published that the mPTP can be completely inhibited in liver mitochondria treated with ADP and CsA (*13*). To determine whether these results could translate to cardiac mitochondria, we treated mitochondria isolated from WT mice hearts to Ca^{2+} boluses following treatment with CsA, ADP, or a combination of both (Fig. 1, A to C). The amount of Ca^{2+} necessary to activate the mPTP increased upon the treatment of either CsA or ADP (Fig. 1B); however, the combination of ADP and CsA led to the complete inhibition of the mPTP indicated by the loss of Ca^{2+} uptake with the simultaneous absence of mitochondrial swelling (Fig. 1, A and C). To confirm

[1]Department of Integrative Physiology, Baylor College of Medicine, Houston, TX, USA. [2]Department of Pediatrics, Cincinnati Children's Hospital and the University of Cincinnati, Cincinnati, OH, USA. [3]The Cardiovascular Research Institute, Baylor College of Medicine, Houston, TX, USA.
*Corresponding author. Email: jason.karch@bcm.edu
†These authors contributed equally to this work.

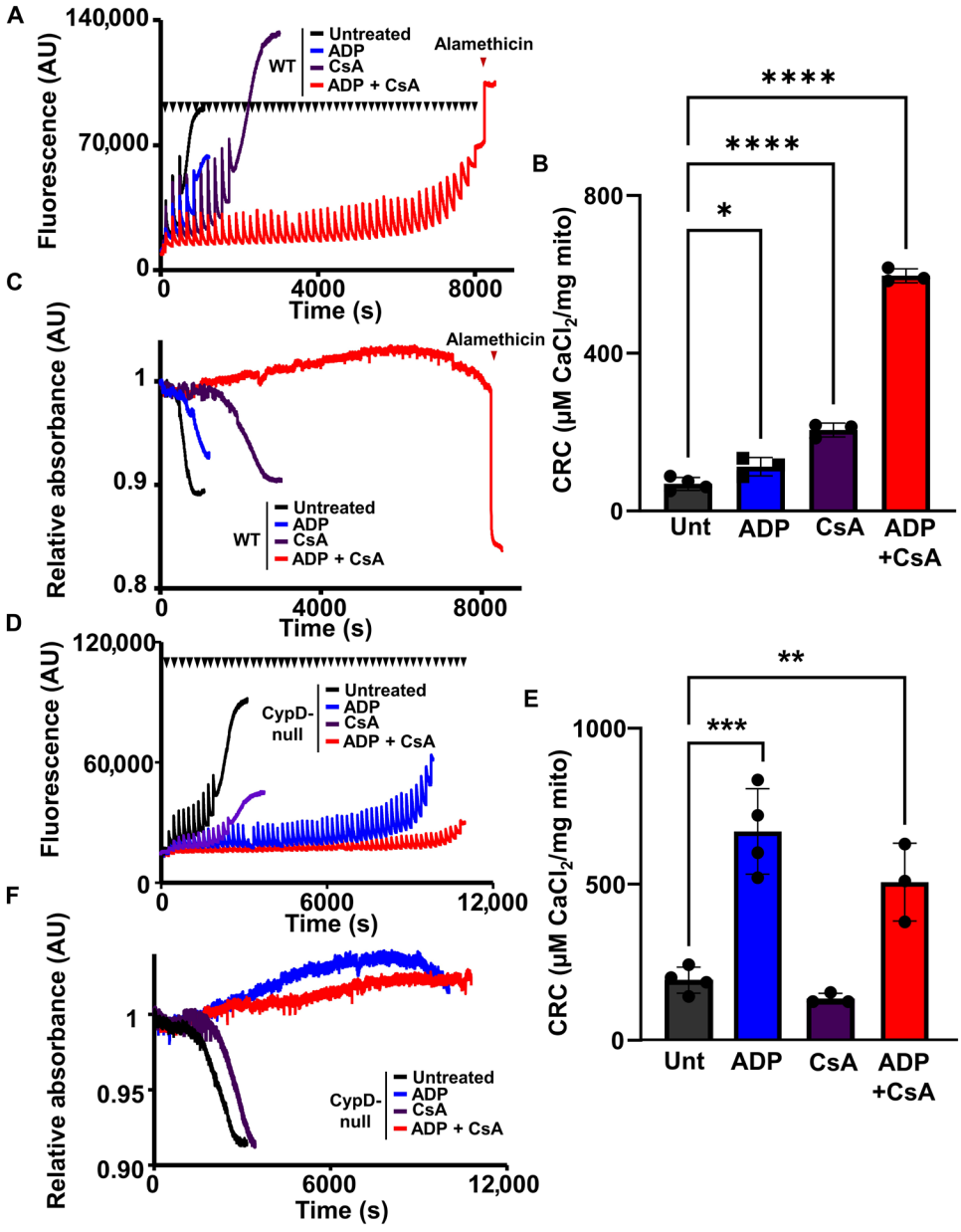

Fig. 1. CypD inhibition or deletion plus ADP treatment synergistically desensitizes mPTP opening in heart mitochondria. (**A**) Representative traces of cardiac mitochondrial CRC assay of WT heart mitochondria untreated (black), pretreated with 300 μM ADP (blue), 2 μM CsA (purple), or a combination of 300 μM ADP and 2 μM CsA (red). Each bolus of calcium (20 μM $CaCl_2$) is indicated by black triangles. The addition of 7 μM alamethicin is indicated by a red triangle. AU, arbitrary units. (**B**) Quantification of (A). (**C**) Representative trace of the mitochondrial swelling assay corresponding to (A). (**D**) Representative traces of cardiac mitochondrial CRC assay of CypD null heart mitochondria untreated (black), pretreated with 300 μM ADP (blue), 2 μM CsA (purple), or a combination of 300 μM ADP and 2 μM CsA (red). Each bolus of calcium (20 μM $CaCl_2$) is indicated by black triangles. (**E**) Quantification of (D). (**F**) Representative trace of corresponding mitochondrial swelling of (D). For all panels of data, $n = 3$. $^*P \leq 0.05$; $^{**}P \leq 0.01$; $^{***}P \leq 0.001$; $^{****}P \leq 0.0001$.

these results genetically, we subjected cardiac mitochondria isolated from *Ppif* $^{-/-}$ mice (*Ppif* is the gene that encodes for CypD) to a similar set of assays treated with or without CsA, ADP, or in combination prior to Ca^{2+} boluses. Because CypD null mitochondria are already desensitized to Ca^{2+}-dependent swelling, their baseline CRC is higher than WT mitochondria and the treatment of CsA did not affect mPTP kinetics (Fig. 1, D to F). Treatment of ADP is able to inhibit Ca^{2+}-induced mPTP opening in CypD null mitochondria similarly to the combination treatment CSA and ADP (Fig. 1, D to F).

To test how the genetic loss of the *Ant* family affects mPTP dynamics and cell death in the heart, we generated mice lacking all ANT isoforms. We crossed previously generated *Slc25A4* $^{-/-}$ (*Ant1* $^{-/-}$), *Slc25a5-LoxP* (fl) (*Ant2* $^{fl/fl}$), *Slc25a31* $^{-/-}$ (*Ant4* $^{-/-}$), and α*MHC-MerCreMer* (MCM) transgenic *mice* to generate *Ant1* $^{-/-}$, *Ant2* $^{fl/fl\text{-}MCM}$, *Ant4* $^{-/-}$ (ANT-cTKO), and controls, *Ant1* $^{-/-}$, *Ant2* $^{fl/fl}$, *Ant4* $^{-/-}$ (ANT2-only). Both groups of these mice and WT mice were subjected to the same tamoxifen regimen, and deletion of the ANT isoforms was confirmed by Western blot analysis (Fig. 2, A to C).

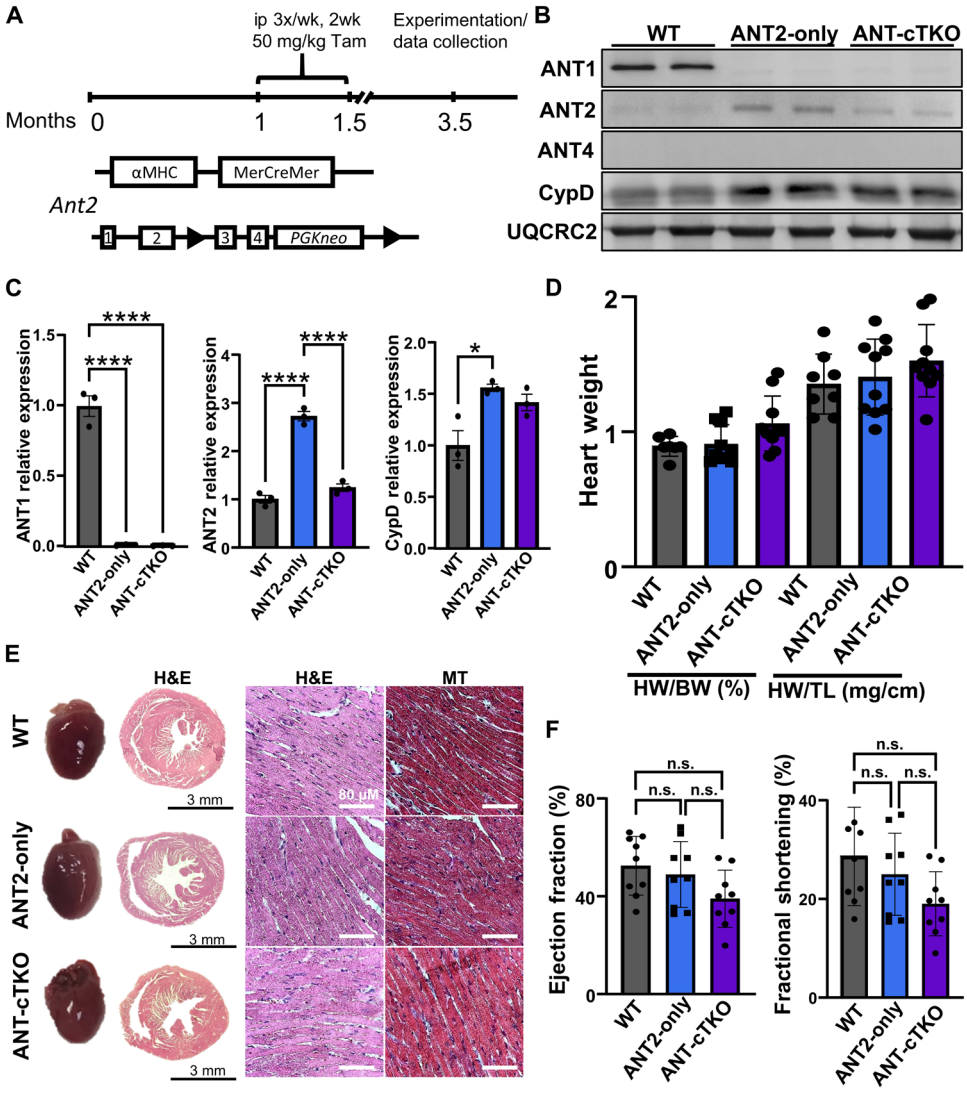

Fig. 2. Baseline characterization of cardiac-specific triple ANT knockout hearts. (**A**) Schematic of genetic generation of *Ant2*$^{fl/fl}$ *αMHC-MerCreMer* mice and tamoxifen (Tam) regimen. ip, intraperitoneally. (**B**) Representative Western blots of ANT1, ANT2, ANT4, CypD, and OXPHOS (UQCRC2, loading control) using WT, ANT2-only, and ANT-cTKO heart mitochondrial protein isolates. (**C**) Protein quantifications of ANT1, ANT2, and CypD over UQCR2 expression relative to the WT sample. (**D**) Quantifications of heart weight over body weight (HW/BW) and heart weight over tibia length (HW/TL) of 3.5-month-old WT (gray), ANT2-only (blue) and ANT-cTKO (purple). (**E**) Representative gross and histological images of H&E and Masson's trichrome staining on cross sections of WT, ANT2-only, and ANT-cTKO hearts. (**F**) Echocardiographic analysis was performed on 3.5-month-old WT, ANT2-only, and ANT-cTKO hearts 2 months after tamoxifen treatment; ejection fraction and fractional shortening are graphed. *$P \leq 0.05$; ****$P \leq 0.0001$; n.s., not significant.

Deletion of *Ant1* and *Ant4* led to a ~3-fold increase in ANT2 in the ANT2-only expressing mice (Fig. 2C). This increase was significantly reduced similarly to WT levels of ANT2 in the ANT-cTKO mice (Fig. 2C). This is likely the lowest achievable level of ANT expression in the heart without inducing lethality or aberrant changes in heart size or function following tamoxifen treatment (Fig. 2, D to F, and fig. S1). Furthermore, no differences were observed in oxygen consumption rates (OCRs) between heart mitochondria isolated from ANT2-only and ANT-cTKO mice and subjected to a mitochondrial stress test (fig. S2).

Once the cardiac ANT null model was established, we isolated heart mitochondria from ANT-cTKO and ANT2-only mice and subjected them to the CRC and mitochondrial swelling assays (Fig. 3, A to L). There were no significant differences between the ANT2-only versus WT mice at baseline; however, the ANT-cTKO mitochondria have significantly increased the CRC (Fig. 3, A to C). When pretreated with ADP, both ANT2-only and ANT-cTKO mitochondria had significantly increased the CRC compared to WT controls (Fig. 3, D to F), However, when pretreated with CsA or a combination of CsA and ADP, ANT-cTKO mitochondria had a significantly higher level of CRC compared to the WT or ANT2-only mitochondria (Fig. 3, G to L). Together, these results show that the deletion of the ANT family leads to mPTP desensitization, which is further exacerbated when CypD is inhibited compared to controls.

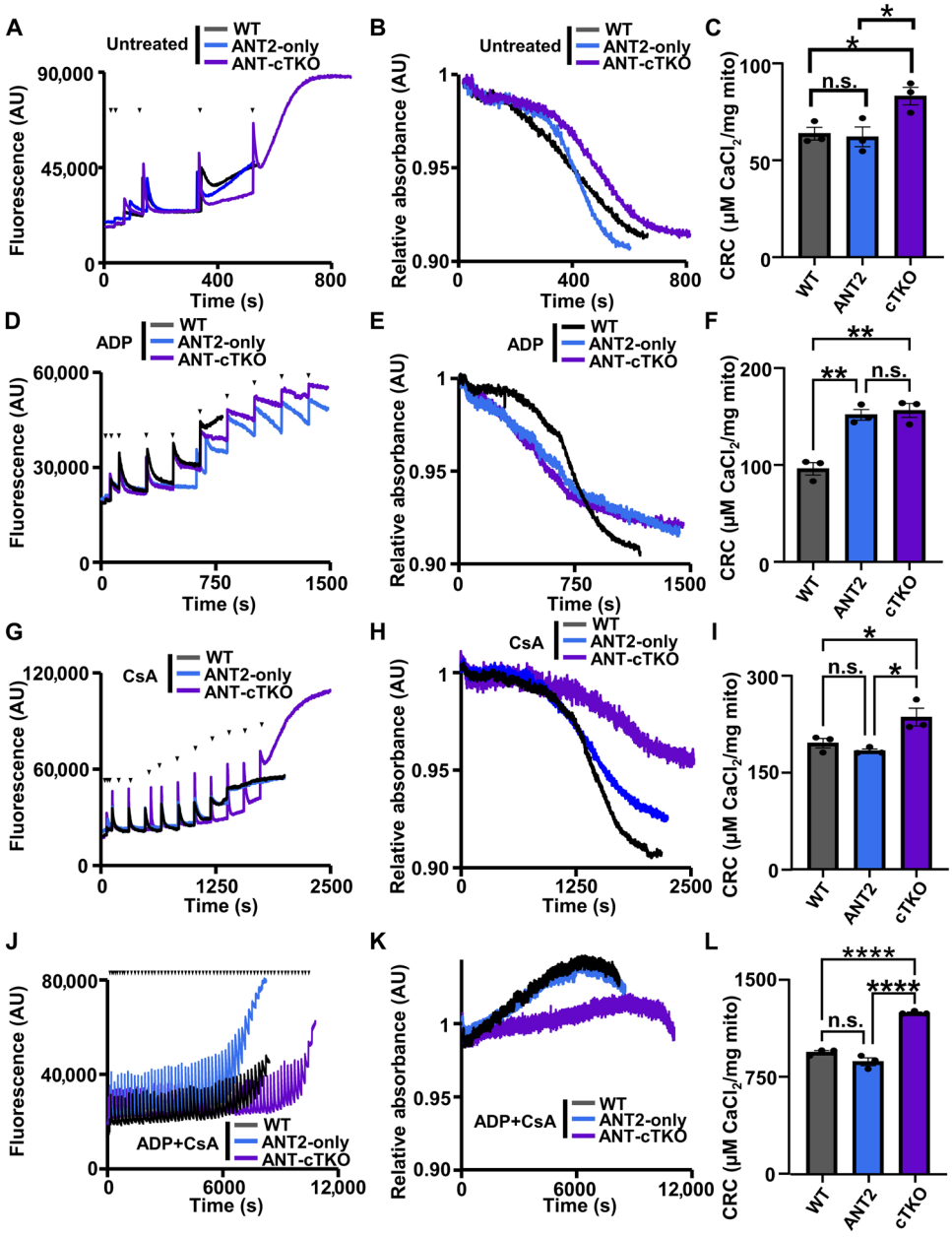

Fig. 3. Mitochondria isolated from ANT cTKO hearts have increased the CRC. (**A**) Representative traces of cardiac mitochondrial CRC assay of WT (black), ANT2-only (blue), and ANT-cTKO (purple) cardiac mitochondria treated with boluses of calcium (20 μM $CaCl_2$) as indicated by black triangles. (**B**) Representative trace of mitochondria swelling corresponding to (A). (**C**) Quantification of the mitochondrial CRC calculated from calcium uptake, as in (A). (**D**) Representative traces of cardiac mitochondrial CRC assay of WT, ANT2-only, and ANT-cTKO cardiac mitochondria pretreated with 300 μM ADP and then treated with boluses of calcium (20 μM $CaCl_2$) as indicated by black triangles. (**E**) Representative trace of mitochondria swelling corresponding to (D). (**F**) Quantification of the mitochondrial CRC calculated from calcium uptake, as in (D). (**G**) Representative traces of cardiac mitochondrial CRC assay of WT, ANT2-only, and ANT-cTKO cardiac mitochondria pretreated with 2 μM CsA and then treated with boluses of calcium (20 μM $CaCl_2$) as indicated by black triangles. (**H**) Representative trace of mitochondria swelling corresponding to (G). (**I**) Quantification of the mitochondrial CRC calculated from calcium uptake, as in (G). (**J**) Representative traces of cardiac mitochondrial CRC assay of WT, ANT2-only, and ANT-cTKO cardiac mitochondria pretreated with 300 μM ADP and 2 μM CsA and then treated with boluses of calcium (20 μM $CaCl_2$) as indicated by black triangles. (**K**) Representative trace of mitochondria swelling corresponding to (J). (**L**) Quantification of the mitochondrial CRC calculated from calcium uptake, as in (J). *$P \leq 0.05$; **$P \leq 0.01$; ****$P \leq 0.0001$; n.s., not significant.

Hearts lacking all isoforms of the ANT family are protective during I/R injury

Because the ANT family positively regulates the mPTP, we hypothesize that the deletion of all isoforms of the ANT family in the heart would be cardioprotective during I/R injury. To test this hypothesis, we subjected WT, ANT2-only, and ANT cTKO mice to 60 min of ischemia via ligation of the left anterior descending (LAD) artery followed by 24 hours of reperfusion. We found that ANT-cTKO hearts had smaller infarct sizes than both WT and ANT2-only hearts (Fig. 4, A to E).

Because dual inhibition of the ANT family and CypD provided the greatest desensitization of the mPTP, we treated WT, ANT2-only, and ANT-cTKO mice with CsA prior to subjecting them to I/R surgery. CsA treatment was able to significantly reduce infarct sizes in WT, ANT2-only, and ANT-cTKO mice (Fig. 5, A to I). However, ANT-cTKO mice treated with CsA had a significantly lower infarct size compared to both WT and ANT2-only mice treated with CsA (Fig. 5, J and K). These data suggest that the ANT-dependent mPTP and CypD-dependent mPTP are both regulators of cell death during I/R injury and that they may lead to mitochondrial dysfunction independently of one another.

Proline-62 within ANT1 is dispensable for mPTP regulation

An untested long-standing hypothesis has been that proline-62 within the first matrix loop of the ANT is the site of CypD isomerization activity to trigger mPTP opening. To test this hypothesis, we generated a novel proline-62 to alanine mutant ANT1 mouse line (ANT1P62A: *Ant1*$^{P62A/P62A}$) using CRISPR-Cas9–mediated gene editing (Fig. 6A). We also introduced an Nru I cut site, for genotyping purposes (Fig. 6A). We confirmed expression of the mutant ANT1 through Western blot analysis (Fig. 6B). Last, we crossed these ANT1P62A mice with the *Ant2*$^{fl/fl}$, *Ant4*$^{-/-}$, and βMHC-Cre transgenic mice to generate *Ant1*$^{P62A/P62A}$, *Ant2*$^{fl/f\text{-}\beta MHC\text{-}Cre}$, *Ant4*$^{-/-}$ (ANT1P62A-only) mice to isolate the mutant ANT1 in the heart. Baseline characterization of these mice revealed no significant differences in heart weight, histological analysis, or functional analysis between WT, ANT1P62A, or ANT1P62A-only mice (Fig. 6, D to G, and fig. S3). Analysis of mitochondrial OCR revealed that ANT1P62A-only expressing mice have overall lower OCR and maximal respiratory capacity (fig. S4).

To determine whether this proline within ANT1 is responsible for regulating mPTP dynamics, we subjected WT and ANT1P62A heart mitochondria to the CRC and swelling assays and found no changes in Ca^{2+}-dependent mPTP opening kinetics (Fig. 7, A and B). The ANT1P62A expressing mutant mitochondria still responded to both CypD inhibition through CsA and ADP to desensitize the mPTP. To rule out the contribution of ANT2 or ANT4, we also subjected the ANT1P62-only heart isolated mitochondria to a similar set of experiments (Fig. 7, C and D). No significant differences were observed in mitochondrial CRC between ANTP62A-only, WT, or ANT1P62A (Fig. 7, E to H). These data suggest that proline-62 within the first matrix loop of the ANT family is dispensable for regulating CypD-dependent mPTP opening or ANT-dependent mPTP opening; therefore, this proline is not the site of CypD isomerization for triggering the mPTP.

Inhibition of CypD reduces the infarct size in ANT1P62A-only expressing mutant mice

To corroborate our ex vivo findings, we subjected WT and ANT1P62A-only cardiac expressing mice to I/R injury with and without CsA treatment. We found that the ANT1P62A-only mice display similar infarct sizes to that of WT mice and that CsA treatment shows similar efficacy in both groups of mice (Fig. 8, A to F). These data combined with the mitochondrial CRC/swelling analysis definitively show that CypD does not regulate the mPTP through proline-62 on ANT1.

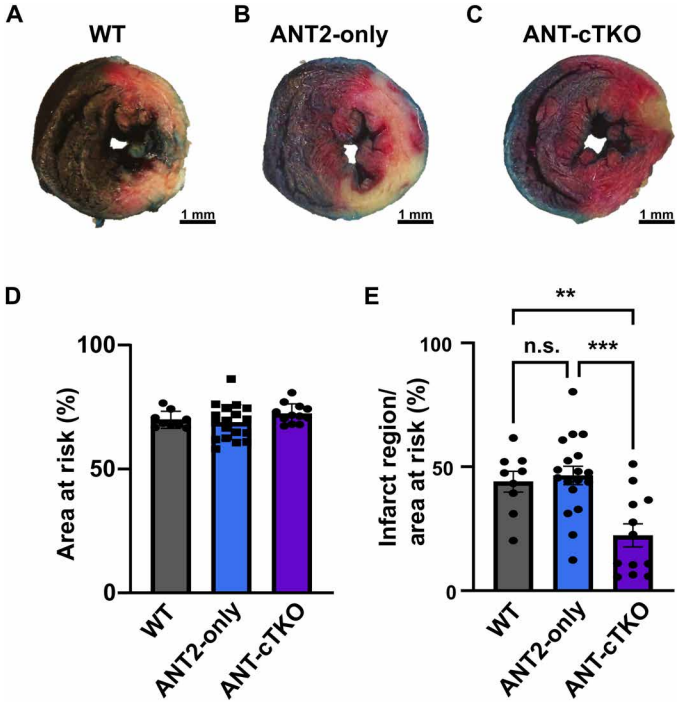

Fig. 4. ANT cTKO hearts are protected from I/R injury. (**A** to **C**) Representative cross section of Evans blue dye and 2,3,5-triphenyltetrazolium chloride stained WT ($n = 9$) (A), ANT2-only ($n = 18$) (B), and ANT cTKO ($n = 12$) (C) hearts after 60 min of ischemia followed by 24 hours of reperfusion. (**D**) Quantification of the area at risk of WT, ANT2-only, and ANT cTKO hearts. (**E**) Quantification of the infarct region over area at risk of WT, ANT2-only, and ANT cTKO hearts. $^{**}P \leq 0.01$; $^{***}P \leq 0.001$.

DISCUSSION

The original model of the mPTP consisted of the ANT family being regulated by CypD to trigger pore opening in the presence of high Ca^{2+} (*13*). When either the ANT family or CypD are genetically deleted, the mPTP still opens but requires more Ca^{2+} to open. Previously, it was shown in liver and skeletal muscle mitochondria that dual inhibition or deletion of both CypD and the ANTs leads to a complete inhibition of the mPTP (*13*, *15*), suggesting that the mPTP requires at least one of these regulators to open. These results support the hypothesis that the mPTP may be composed of two pores. Here, we show that this model is supported in the heart as dual inhibition of the ANTs and CypD provides the strongest inhibitory effect against mPTP opening. Furthermore, we showed that the ANT family positively contributes to infarct size during I/R injury. Notably, deletion of the ANTs from the heart significantly reduced the infarct size in mice that were pretreated with CsA. These data suggest that the ANT family positively contributes to infarct size independently of CypD. CypD-independent mPTP activity through the ANT family may explain why CsA treatment was not effective at

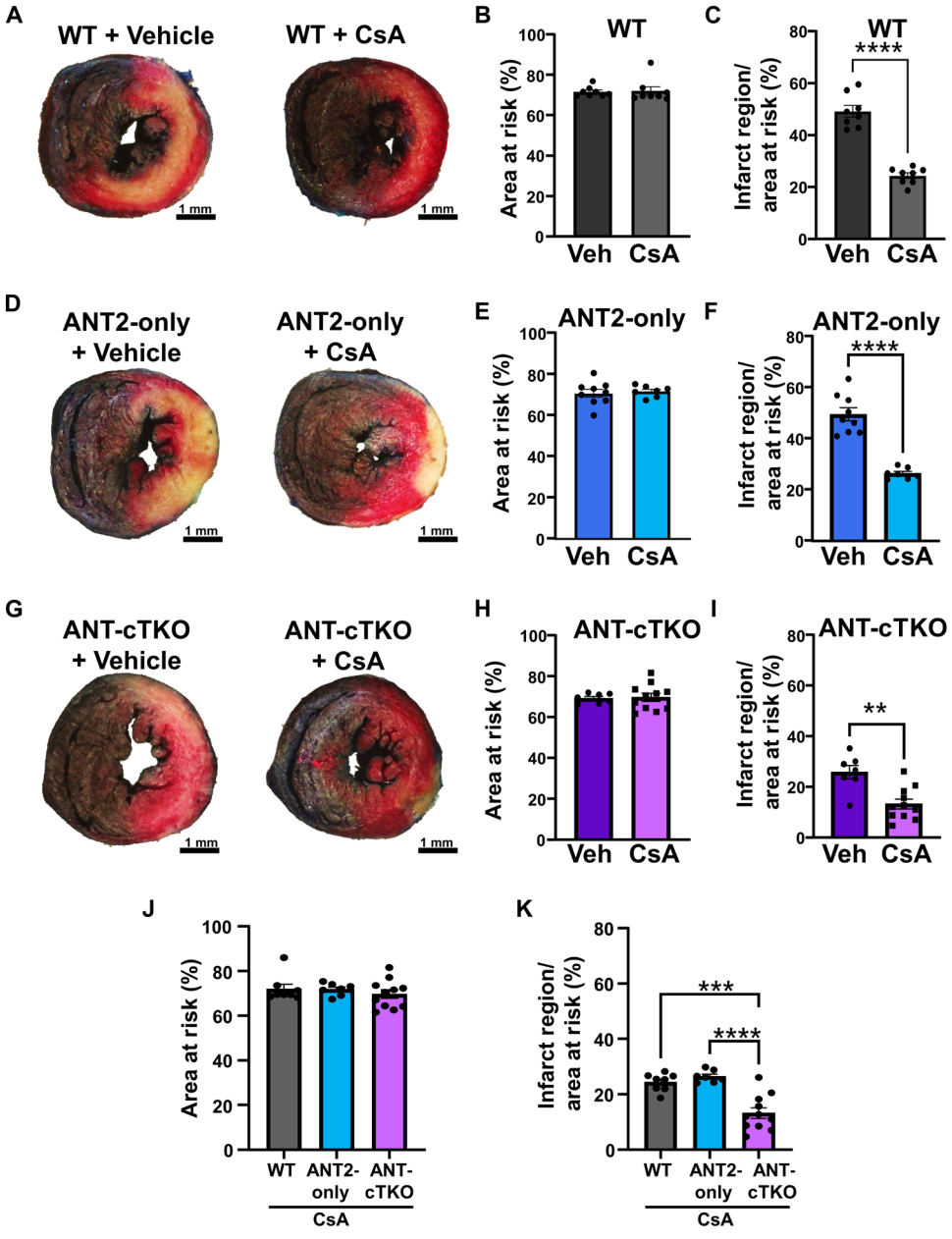

Fig. 5. Inhibition of CypD and deletion of the ANT family conveys additive protection from I/R injury. (**A**) Representative heart cross sections stained with Evans blue dye and 2,3,5-triphenyltetrazolium chloride from WT mice pretreated with vehicle or CsA (10 mg/kg) hearts and then subjected to 60 min of ischemia followed by 24 hours of reperfusion. (**B**) Quantification of the area at risk of (A). (**C**) Quantification of the infarct region over area at risk of (A). (**D**) Representative heart cross sections stained with Evans blue dye and 2,3,5-triphenyltetrazolium chloride from ANT2-only mice pretreated with vehicle or CsA (10 mg/kg) hearts and then subjected to 60 min of ischemia followed by 24 hours of reperfusion. (**E**) Quantification of the area at risk of (D). (**F**) Quantification of the infarct region over area at risk of (D). (**G**) Representative heart cross sections stained with Evans blue dye and 2,3,5-triphenyltetrazolium chloride from ANT-cTKO mice pretreated with vehicle or 10 mg/kg CsA hearts and then subjected to 60 min of ischemia followed by 24 hours of reperfusion. (**H**) Quantification of the area at risk of (G). (**I**) Quantification of the infarct region over area at risk of (G). (**J** and **K**) Quantification of the area at risk (J) and infarct region over area at risk (K) of WT, ANT2-only, and ANT-cTKO mice pretreated with CsA (10 mg/kg) and then subjected to I/R injury. $^{**}P \leq 0.01$; $^{***}P \leq 0.001$; $^{****}P \leq 0.0001$.

improving clinical outcome following a myocardial infarction in human clinical trials (*16*).

Previous studies have shown that CypD and ANTs are binding partners, which suggests that CypD may trigger mPTP opening through the ANT family (*17*, *18*). CypD is a *cis-trans* PPIase, and sanglifehrin A and CsA inhibit its PPIase activity and hamper mPTP opening, which suggests that the PPIase activity is important for mPTP opening (*12*, *19*). In addition, Baines *et al.* showed that the expression of PPIase-dead CypD into CypD-deficient mouse embryonic fibroblasts was unable to restore their sensitivity to H_2O_2-dependent cell death (*7*). In another study, Casin *et al.* generated a CypD isomerase-dead mutant mouse that had increased the

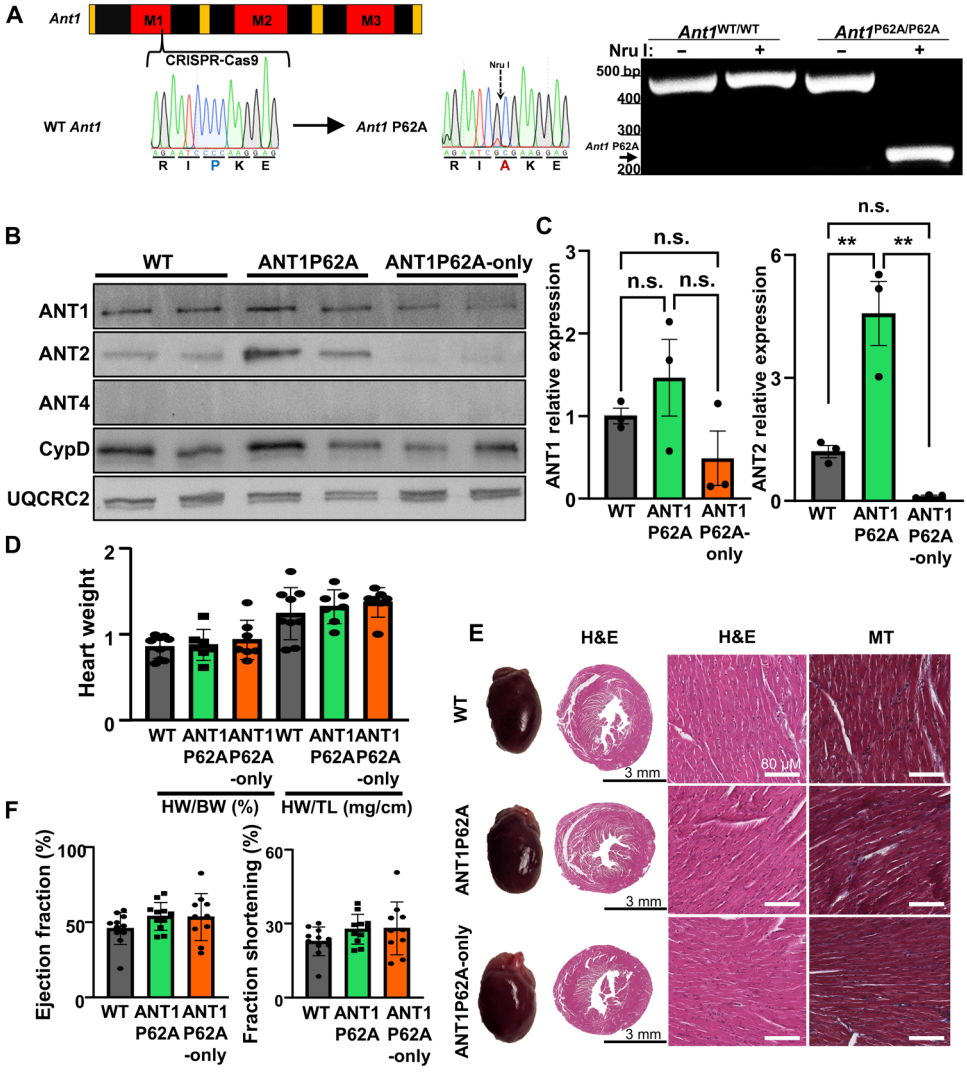

Fig. 6. Generation and baseline characterization of ANT1^{P62A} expressing mice. (**A**) Left: Schematic and sequence analysis of the generation of *Ant1*^{P62A} mutant allele. Right: Genotyping gel for *Ant1* spanning the P62A allele cut with or without Nru I was run using DNA isolated from *Ant1*$^{WT/WT}$ and *Ant1*$^{P62A/P62A}$ mice. bp, base pairs. (**B**) Representative Western blots using cardiac mitochondrial protein isolates from WT, ANT1P62A, and ANT1P62A-only expressing mice of ANT1, ANT2, ANT4, CypD, and UQCRC2 (loading control). (**C**) Protein quantifications of ANT1 and ANT2 over UQCR2 expression relative to the WT sample. (**D**) Quantification of the heart weight to body weight and heart weight to tibia length ratios of WT, ANT1P62A, and ANT1P62A-only mice. (**E**) Representative whole hearts and cross sections of WT, ANT1P62A, and ANT1P62A-only hearts stained with H&E or Masson's trichrome (MT). (**F**) Echocardiographic analysis for ejection fraction and fractional shortening of WT, ANT1P62A, and ANT1P62A-only mice.

mitochondrial CRC and decreased swelling, which suggests that CypD isomerase activity is important for mPTP activation (*20*). Prior investigations have hypothesized that the proline isomerization event targeted by CypD was proline-62 within the first matrix loop of the ANT family (*8*, *12*). Proline-62 is a highly conserved residue in ANT isoforms among mammals and is believed to be important for the matrix-facing state (m-state)–to–cytosol-facing state (c-state) transition of the ANT family; the latter state is associated with mPTP activation (*11*, *21*). Notably, yeast mitochondria have mPTP activity that is unresponsive to CsA treatment and proline-62 is not present in the yeast ANT ortholog (*12*, *22*, *23*). To test whether proline-62 is a regulator of the mPTP, we generated mutant mice that contain an alanine in place of proline-62 of ANT1. In addition, we isolated this mutant isoform of ANT1 in the heart. We found that this proline is dispensable for regulating the mPTP as mPTP kinetics were unchanged in the mutant expressing mitochondria measured by CRC and mitochondrial swelling assays. Furthermore, when we subjected these mice to I/R injury, CsA pretreatment was effective at reducing the infarct size and the infarct size in the vehicle treatment cohort was indistinguishable from WT mice. Together, these data show that proline-62 within ANT1 is not the proline targeted by CypD to trigger mPTP opening.

Although CypD does not activate the mPTP through proline-62 within the ANT family, there may be other candidates to consider. Beyond the ANT family, previous studies have shown that CypD can bind to the ATP Synthase Peripheral Stalk Subunit OSCP (ATPO), leading to a conformational change that results in pore opening at the interface of the F_0 domain (*24*–*26*). In addition, there

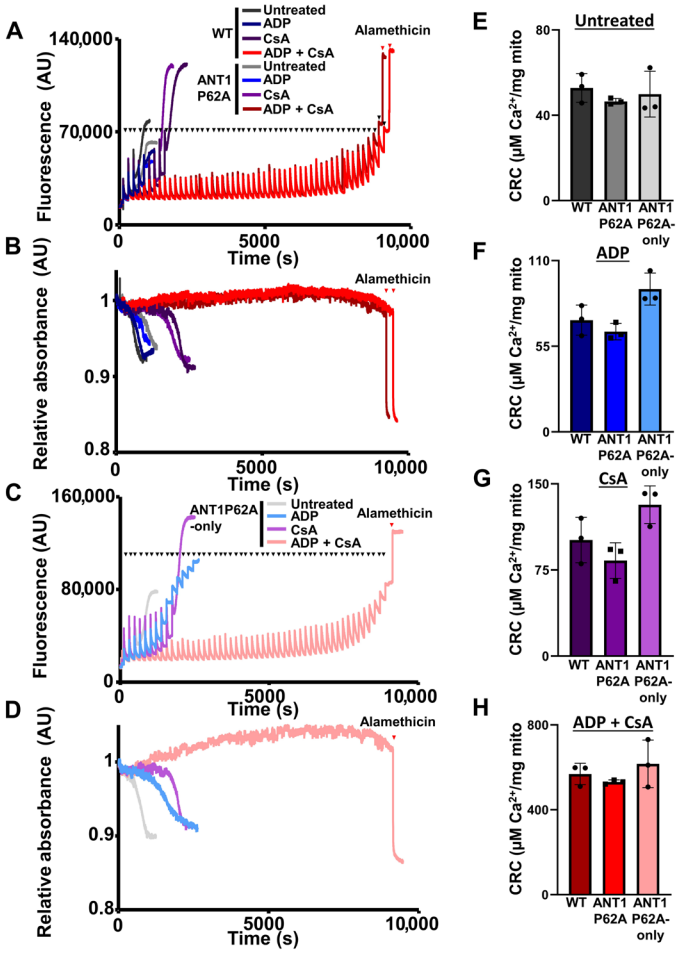

Fig. 7. Proline-62 within ANT1 is dispensable for regulating mitochondrial CRC and swelling. (**A**) Representative mitochondrial calcium uptake of cardiac mitochondria isolated from WT and ANT1P62A expressing mice treated with or without 300 μM ADP and/or 2 μM CsA. Each bolus of calcium is 20 μM $CaCl_2$ and is indicated by black triangles, and red triangles indicate the addition of 7 μM alamethicin. (**B**) Mitochondrial swelling corresponding to (A). (**C**) Representative mitochondrial calcium uptake of cardiac mitochondria isolated from ANT1P62A-only expressing mice treated with or without 300 μM ADP and/or 2 μM CsA. Each bolus of calcium is 20 μM $CaCl_2$ and is indicated by black triangles, and a red triangle indicates the addition of 7 μM alamethicin. (**D**) Mitochondrial swelling corresponding to (C). (**E** to **H**) Quantification of the mitochondrial CRC calculated from (A) and (C). Three independent experiments (n = 3) were performed for every panel.

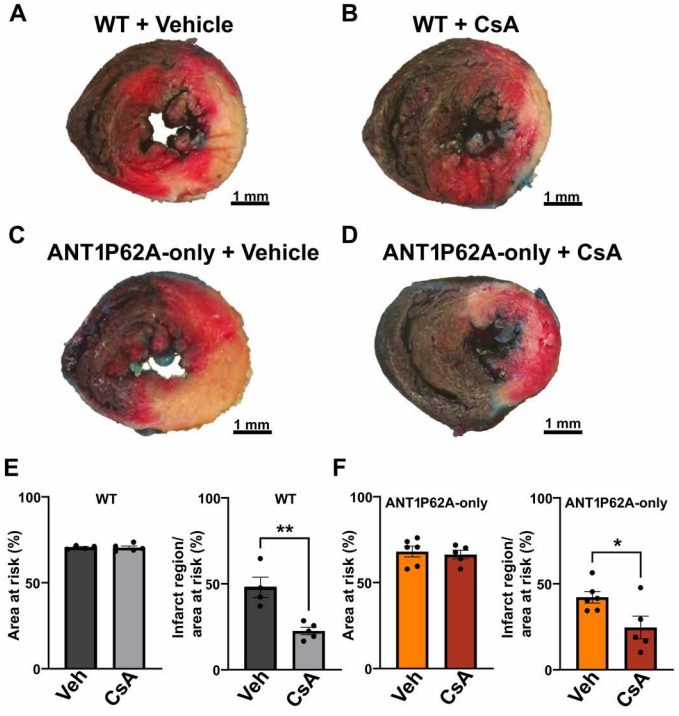

Fig. 8. ANT1P62A-only expressing mice are sensitive to CypD inhibition for reducing the infarct size. (**A** to **D**) Representative cross section of Evans blue dye and 2,3,5-triphenyltetrazolium chloride stained WT and ANT1P62A-only mice treated with vehicle [(A) and (C)] or CsA (10 mg/kg) [(B) and (D)]. Mice were then subjected to cardiac I/R injury by 60 min followed by 24 hours of reperfusion. Scale bars, 1 mm. (**E** and **F**) Quantification of the area at risk and infarct region over area at risk of WT mice (E) and ANT1P62-only mice (F). *$P \leq 0.05$; **$P \leq 0.01$.

is a group of SLC25a carrier proteins that exchange inorganic Mg^{2+} and ATP across the inner mitochondrial membrane that could bind to CypD called the ATP-Mg/P_i (inorganic phosphate) carriers (*27*). These proteins contain EF hands, which are Ca^{2+} regulatory domains and have been shown to modulate Ca^{2+} uptake as well as oxidative stress–induced cell death (*27*, *28*). Moreover, these proteins have conserved prolines within the mitochondrial matrix that could potentially be targeted by CypD. Because the isomerization activity of CypD is critical for mPTP activity, the essential proline targeted by CypD has yet to be identified.

MATERIALS AND METHODS

Animal models

Slc25a4$^{-/-}$ (*Ant1*$^{-/-}$), *Slc25a5*-LoxP (fl) (*Ant2*$^{fl/fl}$), and *Slc25a31*$^{-/-}$ (*Ant4*$^{-/-}$) mice were described previously (*14*, *29*). To generate cardiac-specific deletion of *Ant2*$^{fl/fl}$ mice, we crossed in transgenic mice expressing the tamoxifen-inducible Cre recombinase (MerCreMer) under the control of αMHC (α-myosin heavy chain) promoter transgenic mice (MCM) or transgenic mice expressing the Cre recombinase under the βMHC (β-myosin heavy chain) promoter (*30*, *31*). Ant-triple-null hearts (ANT-cTKO) were generated using *Ant1*$^{-/-}$, *Ant2*$^{fl/fl\text{-}MCM}$, *Ant4*$^{-/-}$ that were injected intraperitoneally with tamoxifen (50 mg/kg) every other day for 2 weeks. Control mice, *Ant1*$^{-/-}$, *Ant2*$^{fl/fl}$, *Ant4*$^{-/-}$ (ANT2-only) littermates not expressing the MCM and WT mice, were subjected to an identical tamoxifen regimen. ANT1P62A mice were generated using CRISPR-Cas9 with cytosolic Cas9 protein embryo microinjections. Mice were generated on a C57BL/6 background and backcrossed with WT C57BL/6 mice seven generations prior to being used for experimentation to eliminate CRISPR-Cas9 off-target gene editing. To generate ANT1P62A mutant-only expressing mice, we crossed the *Ant1*$^{P62A/P62A}$ with *Ant2*$^{fl/fl\text{-}\beta MHC\text{-}Cre}$ and *Ant4*$^{-/-}$ *mice*. All experimental procedures with animals were approved by the Institutional Animal Care and Use Committee (IACUC) of Baylor College of Medicine (protocol IACUC AN-7915). All mice were treated humanely as per compliance with the rules and regulations of animal care and euthanasia under this committee. The

minimal number of mice was used in this study to attain statistical significance based on power analysis calculations.

Heart mitochondrial isolations

Heart ventricles were isolated from WT, *Ppif*$^{-/-}$, ANT-cTKO, ANT2-only, ANT1P62A, or ANT1P62A-only mice and washed in a mitochondrial isolation buffer and then minced into 1- to 2-mm pieces in 1.5 ml mitochondrial isolation buffer (225 mM mannitol, 75 mM sucrose, 5 mM Hepes, and 1 mM EGTA). The tissue was homogenized using a Teflon/glass tissue grinder (~15 strokes). All steps were performed on ice. The homogenates were then centrifuged at 800*g* for 5 min, and the supernatants were then collected and centrifuged at 10,000*g* for 10 min. The supernatants were aspirated, and the pellet was washed with 7 ml of an isolation buffer and then centrifuged at 10,000*g* for 10 min. All centrifugations were performed at 4°C. The pellet from the last spin was suspended in 1 ml of a KCl buffer [125 mM KCl, 20 mM Hepes, 2 mM KH_2PO_4, and 40 μM EGTA (pH 7.2)], and mitochondrial concentration was measured using a Nanodrop.

CRC and mitochondrial swelling assays

Two milligrams of isolated mitochondria was suspended in a total volume of 1 ml consisting of a KCl buffer, 1 mM malic acid (Sigma-Aldrich), 7 mM pyruvate (Sigma-Aldrich), and 50 nM Calcium Green-5N (Invitrogen) in a quartz cuvette, which was placed inside the fluorimeter (PTI QuantaMaster 800, Horiba Scientific). Calcium uptake was measured by fluorescence emission of Calcium Green-5N. Simultaneously, mitochondrial swelling was measured by transmittance light. Some experiments included ADP (300 μM) (Sigma-Aldrich, A2754) or CsA (2 μM) (Sigma-Aldrich, 30024) to desensitize the mPTP. $CaCl_2$ (20 μM) (Sigma-Aldrich, C4901) was added into this system in succession until mPTP opening occurred, indicated by an increase in Calcium Green-5N fluorescence or when mitochondria were saturated with Ca^{2+} and were no longer able to take up further additions of $CaCl_2$, indicated by a stair stacking of Calcium Green-5N fluorescence. CRC was quantified as previously described (*32*).

Western blotting

Mitochondrial pellets were suspended in a radioimmunoprecipitation assay buffer [10 mM tris-HCl (pH 7.49), 100 nM NaCl, 1 mM EDTA, 1 nM EGTA, 1% Triton X-100, 10% glycerol, 0.1% SDS, and 0.5% sodium deoxycholate] containing protease inhibitor cocktails (Roche). Then, these samples were sonicated before centrifugation (21,000*g* for 10 min at 4°C). Afterward, the supernatant fractions were diluted in an SDS sample buffer [250 mM tris-HCl (pH 7.0), 10% SDS, 5% β-mercaptoethanol, 0.02% bromophenol blue, and 30% glycerol] before boiling at 100°C for 5 min. Protein samples were then loaded onto 10 to 15% acrylamide gels and then transferred onto polyvinylidene fluoride transfer membranes (MilliporeSigma). The following primary antibodies were used: ANT1 (Signalway, 32484; 1:500), ANT2 (Cell Signaling Technology; E2B9D; 1:800), ANT4 (Signalway, 40596; 1:800), CypD (Abcam, ab110324; 1:10,000), and Total OXPHOS rodent WB antibody cocktail (OXPHOS) (Abcam; ab110413; 1:10,000). These blots were incubated in their respective secondary antibody, goat anti-mouse Alexa Fluor 488 (Thermo Fisher Scientific, A11029; 1:10,000) for CypD and OXPHOS and goat anti-mouse immunoglobulin G (H+L) (NOVUS, NB7157; 1:10,000) for 2 hours before washing with 1X TBST (20 mM Tris base, 150 mM NaCl, and 0.1% Tween 20) for five washes, each being 5 min long. These blots were incubated in an ECF substrate for 1 min (ANT2) before being imaged using fluorescence (ANT1, ANT4, CypD, and OXPHOS) or ECF (ANT2 and ANT4) and the Thermo Fisher Scientific iBright imaging system.

Mitochondrial stress test

Mitochondria from WT, ANT2-only, ANT-cTKO, ANT1P62A, and ANT1P62A-only mice were isolated in mitochondria isolation buffer [210 mM D-mannitol, 70 mM sucrose, 5 mM Hepes (pH 7.2), 1 mM EGTA, and 0.1% bovine serum albumin (BSA)], and the resulting mitochondrial pellet was resuspended in 500 μl of a mitochondrial assay buffer [220 mM D-mannitol, 70 mM sucrose, 10 mM KH_2PO_4, 5 mM $MgCl_2$, 2 mM Hepes (pH 7.2), 1 mM EGTA, and 0.02% BSA]; mitochondrial concentration was measured using Bradford assay. OCR was analyzed using the Seahorse XF Extracellular Flux Analyzer (Agilent Technologies). Four micrograms of mitochondria per well were plated on XF96 microplates (Agilent Technologies). The mitochondria were then brought up in an isolation buffer with 0.02% BSA and 5 mM pyruvate and 0.5 mM malic acid. Basal respiration was measured before treatments with 500 μM ADP, 10 μM oligomycin, 5 μM carbonyl cyanide *p*-trifluoromethoxyphenylhydrazone, and then 1 μM rotenone (all diluted in an isolation buffer with 5 mM pyruvate and 0.5 mM malic acid).

I/R injury surgery

Mice were placed in an anesthesia induction chamber followed by a nosecone with isoflurane flowing at 5% at 1 to 2% oxygen and locally anesthetized using bupivacaine (1 to 2 mg/kg) prior to a 1-cm ventral incision on the neck to intubate the trachea with more global anesthetic (isoflurane), following a left lateral thoracotomy (1-cm incision) for isolation of the anterolateral heart. Next, the LAD artery was ligated for 60 min via a slipknot followed by 24-hour reperfusion. Mice were then euthanized, and hearts were excised; the sutures were retied around the LAD artery, and hearts were injected and stained with Evans blue dye and then sliced into 1-mm-thick cross sections and incubated and stained with 2,3,5-triphenyltetrazolium to visualize and quantify the area at risk and infarct regions. Before surgery, some mice were intraperitoneally injected with CsA [10 mg/kg; 2.5% CsA (100 mg/kg) in dimethyl sulfoxide (DMSO), 29.5% polyethylene glycol, molecular weight 300 (PEG-300), 5% Tween 80, and 63% saline] or vehicle (2.5% DMSO, 29.5% PEG-300, 5% Tween 80, and 62% saline) for four consecutive days. On the fourth day of injections, mice were subjected to the surgery.

Histological analysis

Hearts were isolated and washed in Hanks' balanced salt solution (MilliporeSigma) and before fixation in 10% formalin overnight at 4°C. Afterward, the hearts were dehydrated in 70% ethanol before embedding in paraffin. Hearts were then sectioned to 5 μm in thickness before being stained with hematoxylin and eosin (H&E) or Masson's trichrome. The slides were then imaged by digital scanning bright-field microscopy using the Aperio AT2 spinning disk confocal microscope.

Echocardiography

Measurements were taken on mice anaesthetized with isoflurane (1.5%) using the VisualSonics F2 Ultrasound 15-MHz microprobe. Both M-mode and B-mode echocardiography were performed. Quantifications were performed using the Vevo LAB program for M-mode in duplicate per mouse and averaged.

Statistical analysis

The data are presented as the mean with the error bars representing the SEM. When comparing two groups, an unpaired two-tailed Student's *t* test was performed, and when comparing multiple groups to the same control, a one-way analysis of variance (ANOVA) was performed followed by a Dunnett's test for post hoc analysis; for multiple comparisons with multiple variables, a two-way ANOVA was performed followed by a Bonferroni test for post hoc analysis using GraphPad Prism. All values were considered statistically significant when $P < 0.05$ as labeled in the figure legends. The sample number of biological replicates for each experiment is indicated as dots within the histograms. Sample number was predetermined using power analysis based on previously generated data. All surgeries, infarct analysis, and echo measurements were performed blinded.

Supplementary Materials

This PDF file includes:

Figs. S1 to S4

REFERENCES AND NOTES

1. K. Konstantinidis, R. S. Whelan, R. N. Kitsis, Mechanisms of cell death in heart disease. *Arterioscler. Thromb. Vasc. Biol.* **32**, 1552–1562 (2012).
2. R. Endlicher, Z. Drahota, K. Štefková, Z. Červinková, O. Kučera, The mitochondrial permeability transition pore—Current knowledge of its structure, function, and regulation, and optimized methods for evaluating its functional state. *Cells* **12**, 1273 (2023).
3. P. Bernardi, C. Gerle, A. P. Halestrap, E. A. Jonas, J. Karch, N. Mnatsakanyan, E. Pavlov, S.-S. Sheu, A. A. Soukas, Identity, structure, and function of the mitochondrial permeability transition pore: Controversies, consensus, recent advances, and future directions. *Cell Death Differ.* **30**, 1869–1885 (2023).
4. J. Karch, J. Q. Kwong, A. R. Burr, M. A. Sargent, J. W. Elrod, P. M. Peixoto, S. Martinez-Caballero, H. Osinska, E. H. Cheng, J. Robbins, K. W. Kinnally, J. D. Molkentin, Bax and Bak function as the outer membrane component of the mitochondrial permeability pore in regulating necrotic cell death in mice. *eLife* **2**, e00772 (2013).
5. P. Patel, A. Mendoza, D. J. Robichaux, M. C. Wang, X. H. Wehrens, J. Karch, Inhibition of the anti-apoptotic Bcl-2 family by BH3 mimetics sensitize the mitochondrial permeability transition pore through Bax and Bak. *Front. Cell Dev. Biol.* **9**, 765973 (2021).
6. G. Amanakis, E. Murphy, Cyclophilin D: An integrator of mitochondrial function. *Front. Physiol.* **11**, 595 (2020).
7. C. P. Baines, R. A. Kaiser, N. H. Purcell, N. S. Blair, H. Osinska, M. A. Hambleton, E. W. Brunskill, M. R. Sayen, R. A. Gottlieb, G. W. Dorn, J. Robbins, J. D. Molkentin, Loss of cyclophilin D reveals a critical role for mitochondrial permeability transition in cell death. *Nature* **434**, 658–662 (2005).
8. A. P. Halestrap, A. M. Davidson, Inhibition of Ca^{2+}-induced large-amplitude swelling of liver and heart mitochondria by cyclosporin is probably caused by the inhibitor binding to mitochondrial-matrix peptidyl-prolyl cis-trans isomerase and preventing it interacting with the adenine nucleotide translocase. *Biochem. J.* **268**, 153–160 (1990).
9. E. Hochhauser, S. Kivity, D. Offen, N. Maulik, H. Otani, Y. Barhum, H. Pannet, V. Shneyvays, A. Shainberg, V. Goldshtaub, A. Tobar, B. A. Vidne, Bax ablation protects against myocardial ischemia-reperfusion injury in transgenic mice. *Am. J. Physiol. Heart Circ. Physiol.* **284**, H2351–H2359 (2003).
10. E. Hochhauser, Y. Cheporko, N. Yasovich, L. Pinchas, D. Offen, Y. Barhum, H. Pannet, A. Tobar, B. Vidne, E. Birk, Bax deficiency reduces infarct size and improves long-term function after myocardial infarction. *Cell Biochem. Biophys.* **47**, 11–20 (2007).
11. M. J. Bround, D. M. Bers, J. D. Molkentin, A 20/20 view of ANT function in mitochondrial biology and necrotic cell death. *J. Mol. Cell. Cardiol.* **144**, A3–A13 (2020).
12. A. P. Halestrap, C. Brenner, The adenine nucleotide translocase: A central component of the mitochondrial permeability transition pore and key player in cell death. *Curr. Med. Chem.* **10**, 1507–1525 (2003).
13. J. Karch, M. J. Bround, H. Khalil, M. A. Sargent, N. Latchman, N. Terada, P. M. Peixoto, J. D. Molkentin, Inhibition of mitochondrial permeability transition by deletion of the ANT family and CypD. *Sci. Adv.* **5**, eaaw4597 (2019).
14. J. E. Kokoszka, K. G. Waymire, S. E. Levy, J. E. Sligh, J. Cai, D. P. Jones, G. R. MacGregor, D. C. Wallace, The ADP/ATP translocator is not essential for the mitochondrial permeability transition pore. *Nature* **427**, 461–465 (2004).
15. M. J. Bround, J. R. Havens, A. J. York, M. A. Sargent, J. Karch, J. D. Molkentin, ANT-dependent MPTP underlies necrotic myofiber death in muscular dystrophy. *Sci. Adv.* **9**, eadi2767 (2023).
16. T.-T. Cung, O. Morel, G. Cayla, G. Rioufol, D. Garcia-Dorado, D. Angoulvant, E. Bonnefoy-Cudraz, P. Guérin, M. Elbaz, N. Delarche, P. Coste, G. Vanzetto, M. Metge, J.-F. Aupetit, B. Jouve, P. Motreff, C. Tron, J.-N. Labeque, P. G. Steg, Y. Cottin, G. Range, J. Clerc, M. J. Claeys, P. Coussement, F. Prunier, F. Moulin, O. Roth, L. Belle, P. Dubois, P. Barragan, M. Gilard, C. Piot, P. Colin, F. De Poli, M.-C. Morice, O. Ider, J.-L. Dubois-Randé, T. Unterseeh, H. L. Breton, T. Béard, D. Blanchard, G. Grollier, V. Malquarti, P. Staat, A. Sudre, E. Elmer, M. J. Hansson, C. Bergerot, I. Boussaha, C. Jossan, G. Derumeaux, N. Mewton, M. Ovize, Cyclosporine before PCI in patients with acute myocardial infarction. *N. Engl. J. Med.* **373**, 1021–1031 (2015).
17. K. Woodfield, A. Rück, D. Brdiczka, A. P. Halestrap, Direct demonstration of a specific interaction between cyclophilin-D and the adenine nucleotide translocase confirms their role in the mitochondrial permeability transition. *Biochem. J.* **336**, 287–290 (1998).
18. M. Crompton, S. Virji, J. M. Ward, Cyclophilin-D binds strongly to complexes of the voltage-dependent anion channel and the adenine nucleotide translocase to form the permeability transition pore. *Eur. J. Biochem.* **258**, 729–735 (1998).
19. S. J. Clarke, G. P. McStay, A. P. Halestrap, Sanglifehrin A acts as a potent inhibitor of the mitochondrial permeability transition and reperfusion injury of the heart by binding to cyclophilin-D at a different site from cyclosporin A. *J. Biol. Chem.* **277**, 34793–34799 (2002).
20. K. M. Casin, M. Bustamante, G. Amanakis, J. Sun, C. Liu, R. N. Kitsis, E. Murphy, Loss of cyclophilin D prolyl isomerase activity desensitizes mitochondrial permeability transition pore opening in isolated cardiac mitochondria, but does not protect in myocardial ischemia-reperfusion injury. *J. Mol. Cell. Cardiol.* **183**, 67–69 (2023).
21. A. L. Cozens, M. J. Runswick, J. E. Walker, DNA sequences of two expressed nuclear genes for human mitochondrial ADP/ATP translocase. *J. Mol. Biol.* **206**, 261–280 (1989).
22. J. Kolarov, N. Kolarova, N. Nelson, A third ADP/ATP translocator gene in yeast. *J. Biol. Chem.* **265**, 12711–12716 (1990).
23. A. P. Halestrap, K.-Y. Woodfield, C. P. Connern, Oxidative stress, thiol reagents, and membrane potential modulate the mitochondrial permeability transition by affecting nucleotide binding to the adenine nucleotide translocase. *J. Biol. Chem.* **272**, 3346–3354 (1997).
24. C. Chinopoulos, C. Konràd, G. Kiss, E. Metelkin, B. Töröcsik, S. F. Zhang, A. A. Starkov, Modulation of F_0F1-ATP synthase activity by cyclophilin D regulates matrix adenine nucleotide levels. *FEBS J.* **278**, 1112–1125 (2011).
25. P. Bernardi, M. Carraro, G. Lippe, The mitochondrial permeability transition: Recent progress and open questions. *FEBS J.* **289**, 7051–7074 (2022).
26. E. Murphy, Cyclophilin D regulation of the mitochondrial permeability transition pore. *Curr. Opin. Physiol.* **25**, 100486 (2022).
27. J. J. Ruprecht, E. R. Kunji, The SLC25 mitochondrial carrier family: Structure and mechanism. *Trends Biochem. Sci.* **45**, 244–258 (2020).
28. N. E. Hoffman, H. C. Chandramoorthy, S. Shanmughapriya, X. Q. Zhang, S. Vallem, P. J. Doonan, K. Malliankaraman, S. Guo, S. Rajan, J. W. Elrod, W. J. Koch, J. Y. Cheung, M. Madesh, SLC25A23 augments mitochondrial Ca^{2+} uptake, interacts with MCU, and induces oxidative stress–mediated cell death. *Mol. Biol. Cell* **25**, 936–947 (2014).
29. J. V. Brower, C. H. Lim, M. Jorgensen, S. P. Oh, N. Terada, Adenine nucleotide translocase 4 deficiency leads to early meiotic arrest of murine male germ cells. *Reproduction* **138**, 463–470 (2009).
30. J. D. Molkentin, S. M. Jobe, B. E. Markham, α-myosin heavy chain gene regulation: Delineation and characterization of the cardiac muscle-specific enhancer and muscle-specific promoter. *J. Mol. Cell. Cardiol.* **28**, 1211–1225 (1996).
31. C. E. Wright, F. Haddad, A. Qin, P. Bodell, K. Baldwin, In vivo regulation of β-MHC gene in rodent heart: Role of T3 and evidence for an upstream enhancer. *Am. J. Physiol. Heart Circ. Physiol.* **276**, C883–C891 (1999).
32. A. M. Mendoza, J. Karch, "Simultaneous acquisition of mitochondrial calcium retention capacity and swelling to measure permeability transition sensitivity" in *Mitochondria: Methods and Protocols* (Springer, 2022), pp. 129–140.

Acknowledgments

Funding: This work was supported by the National Heart, Lung, and Blood Institute of the National Institutes of Health [grant R01HL150031 (to J.K.)] and by the Genetically Engineered Rodent Model Core at BCM. The GERM Core is funded in part by the National Institutes of Health Cancer Center Grant (P30 CA125123). **Author contributions:** Conceptualization: J.K. Methodology: J.D.M. and J.K. Investigation: P.P., A.M., Da.R., De.R., and J.K. Visualization: P.P., A.M., De.R., ad J.K. Supervision: J.K. Writing—original draft: P.P. and J.K. Writing—review and editing: P.P., A.M., De.R., and J.K. **Competing interests:** The authors declare that they have no competing interests. **Data and materials availability:** All data needed to evaluate the conclusions in the paper are present in the paper and/or the Supplementary Materials. The ANT1P62A mutant mice can be provided by Baylor College of Medicine pending scientific review and a completed material transfer agreement. Requests for the ANT1P62A mutant mice should be submitted to Jason.karch@bcm.edu.

Submitted 9 April 2024
Accepted 4 November 2024
Published 11 December 2024
10.1126/sciadv.adp7444